Calculation of Electromagnetic Scattering via Boundary Variations and Analytic Continuation

OSCAR P. BRUNO
Applied Mathematics, California Institute of Technology
Pasadena, CA 91125 bruno@ama.caltech.edu

FERNANDO REITICH
Department of Mathematics and Center for Research in Scientific Computation,
North Carolina State University
Raleigh, NC 27695 reitich@math.ncsu.edu

Abstract

In this paper we review a numerical method we introduced recently for the solution of problems of electromagnetic scattering. Based on variations of the boundaries of the scatterers and analytic continuation, our approach yields algorithms which are applicable to a wide variety of scattering configurations. We discuss some recent applications of this method to scattering by diffraction gratings and by large two-dimensional bounded bodies, and we present results of new applications to three-dimensional gratings containing corners and edges. In many cases of practical interest our algorithms give numerical results which are several orders of magnitude more accurate than those given by classical methods.

1 Introduction

The problem of calculating the electromagnetic scattering produced by obstacles is one of utmost importance in science and engineering. Much of what we "see" –be it through visible light or x-rays, radio or microwaves– reaches us through a complicated combination of phenomena among which scattering is, in most cases, an essential element. In accordance with the substantial significance of scattering, a great deal of effort has been devoted in the last century to treating a variety of instances of this challenging mathematical problem. Among the many resulting contributions we mention exact solutions for simple geometries, high and low frequency approximations (Kirchoff and Rayleigh solutions) and rigorous numerical methods.

Consideration of exact solutions associated with simple scatterers, such as a semi-space or a spherical particle, has lead to fundamental understanding in optics and electromagnetism. Many problems encountered in practice, on the other hand, are associated with geometries for which exact solutions cannot be found and simple approximations cannot be used, and which must therefore be dealt with by means of numerical solution of Maxwell's equations. This is the case, for example, for scattering configurations in the resonance region —where the wavelength of radiation is comparable with the size of the obstacle. The collection of scattering solvers which have been devised to treat these problems includes methods based on the solution of integral equations [17, 27, 35, 25, 22, 11] and methods based on finite elements or finite differences approximations [3, 14, 19, 28]. In this paper we review a method we introduced recently. Based on variations of the boundaries of the scatterers and analytic continuation, our new perturbative approach leads to algorithms which are applicable to a wide variety of scattering configurations. In many cases of practical interest these algorithms yield numerical results which are several orders of magnitude more accurate than those given by classical methods — see §5.

For several decades perturbation methods have been considered inadequate for the treatment of problems of wave scattering, and only few of the many discussions, mainly in the area scattering by corrugated surfaces, have been based on perturbative techniques. Low order perturbative approaches include the first order calculation of Rayleigh [31]; see [37] for a more recent contribution. As for higher order methods we mention the work of Meecham [26], Greffet and Maassarani [16] and Lopez, Yndurain and García [20]. Low order methods are only appropriate for very small departures from an exactly solvable geometry, and they cannot be applied to scatterers in the resonance region [23, 33]. The high order approach of Meecham produces the scattering from a

corrugated surface as a Neumann series whose n-th term is given by an n-fold convolution of the Green's function. This method, which Meecham did not implement numerically, was thought to be mathematically incorrect [34] and dismissed. Later, Greffet and Maassarani studied these perturbations expansions and proposed that their convergence is tied with the validity of the Rayleigh hypothesis [16, pp. 1488–1489]; we now know [8] that such a link does not exist. Lopez, Yndurain and García, on the other hand, pointed out certain limitations in convergence. They proposed these limitations where caused by *poles of the fields in the negative real axis of the perturbation parameter plane*. As indicated below, we have shown poles do not occur anywhere in the real parameter axis. And, further, we have established that the observed limitations in convergence can be effectively overcome by use of adequate methods of analytic continuation.

(The most comprehensive objection to perturbative approaches is that of Uretsky [34, p. 411], who conjectured that the electromagnetic field for a corrugated surface does not continue analytically to the fields for a flat interface. As a specific example of this conjecture this author proposed an infinite sinusoidal corrugation of a plane. Uretsky's conjecture was based on a certain integral expression, related to the fields, which appears to become meaningless as the groove depth takes on complex values. He thus suggested that series expansions in powers of the parameters controlling the shape of the scatterers could not be used in the solution of the corresponding scattering problems. As we have shown, however, the field *does* vary analytically with respect to boundary variations [6].)

In this paper we review our theory and discuss the performance of our algorithms in a number of two- and three-dimensional configurations. In particular, we present results of new applications to two-dimensional bounded obstacles and to three-dimensional gratings containing edges and corners. All of our numerical results are accompanied by reliable error estimates.

The applications to non-smooth three-dimensional gratings given here required the introduction of a class of numerical devices which will also be needed in our forthcoming applications to three-dimensional bounded-obstacle problems, see §3.3. These methods have cleared the way for the application of our perturbative approach to bounded three-dimensional scatterers. We expect the performance of our algorithms in these problems will be of a quality comparable to the one they exhibit in the various configurations considered in this paper.

2 Preliminaries

2.1 Maxwell equations

Consider a scattering configuration in which space is divided in two regions Ω^+ and Ω^- containing two different materials, such as air and a metal, of respective dielectric constants ϵ^+ and ϵ^-. The permeability of both materials is assumed to equal μ_0, the permeability of vacuum. In the cases we consider, the region Ω^+ is of infinite extent; the scatterer Ω^-, on the other hand, may be bounded or unbounded.

We wish to determine the pattern of diffraction that occurs when an electromagnetic plane wave

$$\vec{E}^i = \vec{A}e^{i(\alpha x_1+\beta x_2-\gamma x_3)-i\omega t}$$
$$\vec{H}^i = \vec{B}e^{i(\alpha x_1+\beta x_2-\gamma x_3)-i\omega t}$$

impinges upon Ω^-. Here, denoting by $\vec{k} = (\alpha, \beta, -\gamma)$ the wavevector, we have

$$\vec{A}\cdot\vec{k} = 0 \text{ and } \vec{B} = \frac{1}{\omega\mu_0}\vec{k}\times\vec{A}. \tag{1}$$

Dropping the factor $e^{-i\omega t}$, the time harmonic Maxwell equations for the total fields read

$$\nabla\times\vec{E} = i\omega\mu_0\vec{H} \ , \ \nabla\cdot\vec{E} = 0 \ ,$$
$$\nabla\times\vec{H} = -i\omega\epsilon\vec{E} \ , \ \nabla\cdot\vec{H} = 0 \ . \tag{2}$$

In particular the electromagnetic field

$$v = (\vec{E}, \vec{H}) \tag{3}$$

satisfies the Helmholtz equations

$$\Delta v + (k^\pm)^2 v = 0 \text{ in } \Omega^\pm, \tag{4}$$

where $k^\pm = \omega\sqrt{\mu_0\epsilon^\pm}$. The total electric and magnetic fields are given by

$$\vec{E} = \vec{E}^{out} = \vec{E}^i + \vec{E}^+ \ , \ \vec{H} = \vec{H}^i + \vec{H}^+ \text{ in } \Omega^+ \text{ and}$$
$$\vec{E} = \vec{E}^{in} = \vec{E}^- \ , \ \vec{H} = \vec{H}^- \text{ in } \Omega^-,$$

where $(\vec{E}^+, \vec{H}^+)$ and $(\vec{E}^-, \vec{H}^-)$ are the reflected and refracted fields, respectively. At the interface

$$\Gamma = \partial\Omega^+ = \partial\Omega^-$$

the field satisfies the transmission conditions

$$n\times(\vec{E}^{out}-\vec{E}^{in}) = 0 \ , \ n\times(\vec{H}^{out}-\vec{H}^{in}) = 0 \text{ on } \Gamma, \tag{5}$$

where n is normal to Γ. In case the region Ω^- is filled by a perfect conductor the refracted fields vanish and the boundary conditions reduce to

$$n\times\vec{E}^{out} = n\times(\vec{E}^i+\vec{E}^+) = 0 \text{ on } \Gamma \ . \tag{6}$$

Finally the field satisfies conditions of radiation at infinity, expressing the outgoing character of the scattered waves, which can be stated either in terms of the eigenfunctions expansions of §2.2, or, alternatively, in terms of the decay of the field at infinity; see e.g. [4, 18, 29].

In the two dimensional case in which Ω^- is a cylinder and $\beta = 0$, the fields $\vec{E}$ and $\vec{H}$ are independent of x_2 and the system of equations (2),(5) (or (2),(6)) can be reduced to a pair of decoupled equations for two scalar unknowns [21]. Indeed, the functions $u_1(x_1, x_3)$ and $u_2(x_1, x_3)$ equal to the transverse components E_{x_2} (Field Transverse Electric, TE) and H_{x_2} (Field Transverse Magnetic, TM), which satisfy equation (4), determine completely the electromagnetic field through equations (2). The boundary conditions (6), (5) can be translated into appropriate boundary conditions for the unknowns u_i. In case Ω^- contains a perfect conductor, we have

$$u_1 = -e^{i\alpha x_1 - i\gamma x_3} \quad \text{and} \tag{7}$$

$$\frac{\partial u_2}{\partial n} = -\frac{\partial}{\partial n}\left(e^{i\alpha x_1 - i\gamma x_3}\right) \text{ on } \Gamma. \tag{8}$$

In case Ω^- contains a finitely conducting metal or dielectric u_1 satisfies the transmission conditions

$$\begin{aligned} u_1^+ - u_1^- &= -e^{i\alpha x_1 - i\gamma x_3} \ , \text{ and} \\ \frac{\partial u_1^+}{\partial n} - \frac{\partial u_1^-}{\partial n} &= -\frac{\partial}{\partial n}\left(e^{i\alpha x_1 - i\gamma x_3}\right) \quad \text{on } \Gamma, \end{aligned} \tag{9}$$

while u_2 satisfies

$$\begin{aligned} u_2^+ - u_2^- &= -e^{i\alpha x_1 - i\gamma x_3} \ , \text{ and} \\ \frac{\partial u_2^+}{\partial n} - \left(\frac{k^+}{k^-}\right)^2 \frac{\partial u_2^-}{\partial n} &= -\frac{\partial}{\partial n}\left(e^{i\alpha x_1 - i\gamma x_3}\right) \text{ on } \Gamma. \end{aligned} \tag{10}$$

2.2 Eigenfunction expansions

In addition to Taylor series, our analytic approach is based on the series expansions of the electromagnetic field which result from separation of variables. Such expansions, which we review briefly later in this section, are most frequently found in solutions associated with simple objects such as a circle, a sphere or a semispace. For such simple scatterers the functions resulting from restriction of the separated solutions to the scattering boundaries form a complete orthonormal system, and thus boundary conditions can easily be accounted for by means of Fourier analysis.

It is interesting to note, however, that expansions in series of separated variables may be useful even when their restrictions to the boundary of the scatterer do not form an orthogonal system. The first occurrence of an approach of this type can be found in the work of Rayleigh [31]. After evaluating such expansions at the scattering boundaries, this author used appropriate approximations and found first order corrections to the scattered field for geometries which result from small perturbations from an exactly solvable one. With the advent of computers attempts were made to extend Rayleigh's approach of evaluating series expansions at the boundary of the obstacles to general scattering solvers which do not assume small departures from an exact geometry. These attempts did not succeed since, indeed, the series may not converge at the obstacle boundaries, that is, Rayleigh's hypothesis may not be satisfied. This fact was first established by Petit and Cadilhac [30] by consideration of a sinusoidal corrugation on a plane.

Our method, whose theoretical validity for *arbitrarily large* perturbations has been established [6], is not unrelated to Rayleigh's hypothesis. Indeed, we showed Rayleigh's hypothesis is valid for sufficiently small perturbations. Whereas these "sufficiently small" perturbations may be too small to be of practical utility, they are certainly sufficient to allow for calculation of the high order derivatives (with respect to boundary perturbations) that we need in our numerics; our algorithm then proceeds via analytic continuation.

Let us now review some eigenfunction expansions we will use. In two dimensions and outside a circular cylinder, for example, any solution to the two-dimensional Helmholtz equation is given by an expansion of the form

$$u(\rho, \theta) = \sum_{r=-\infty}^{\infty} B_r (-i)^r H_r^{(1)}(k\rho) e^{ir\theta}. \tag{11}$$

where ρ and θ are polar coordinates, and where $H_r^{(1)}$ denotes the first Hankel function of order r. The principle of conservation of energy can be given a simple form in terms of the amplitudes B_r in this expansion. Indeed, if u in (11) is a solution to a scattering problem from a perfectly conducting obstacle *of any shape* we then have

$$\sum_r |B_r|^2 + \mathrm{Re}\left(\sum_r B_r\right) = 0. \tag{12}$$

Relation (12), which holds irrespective of whether or not the series (11) converges at the boundary of the obstacle, can be made into a useful estimator for errors in the numerical calculation of the fields, see §5.

For a solution in three dimensional space and outside a sphere we have

$$E^+(R, \theta, \phi) = \sum_{r=0}^{\infty} \sum_{s=-r}^{r} \tilde{B}_{r,s} h_r^{(1)}(kR) P_r^s(\cos(\theta)) e^{is\phi} \tag{13}$$

where (R, θ, ϕ) are spherical coordinates, P_r^s are the Legendre functions of the first kind and $h_r^{(1)}$ are the first spherical Hankel functions [18].

Finally let us consider scatterers which are given by a biperiodic corrugation of a plane

$$\Omega^- = \{z < f(x_1, x_2)\}, \tag{14}$$

where f is a biperiodic function of periods d_1 and d_2 in the variables x_1 and x_2 , respectively. The periodicity of the structure implies that the fields must be (α, β) quasi-periodic, i.e., they must verify equations of the form

$$v(x_1 + d_1, x_2, x_3) = e^{i\alpha d_1} v(x_1, x_2, x_3) \text{ and}$$

$$v(x_1, x_2 + d_2, x_3) = e^{i\beta d_2} v(x_1, x_2, x_3).$$

In this case, separation of variables leads to expansions of the form

$$\vec{E}^{\pm} = \sum_{r=-\infty}^{\infty} \sum_{s=-\infty}^{\infty} \vec{B}^{\pm}_{r,s} e^{i\alpha_r x_1 + i\beta_s x_2 \pm i\gamma^{\pm}_{r,s} x_3}. \tag{15}$$

The expansion for $\vec{E}^+$ (resp. $\vec{E}^-$) converges to the field in the region $\{x_3 > \max(f(x_1, x_2))\}$ (resp. $\{x_3 < \min(f(x_1, x_2))\}$). Here we have put

$$\alpha_r = \alpha + rK_1 \ , \ \beta_s = \beta + sK_2 \ , \ \alpha_r^2 + \beta_s^2 + (\gamma^{\pm}_{r,s})^2 = (k^{\pm})^2 \tag{16}$$

where $\gamma^{\pm}_{r,s}$ is determined by $\mathrm{Im}(\gamma^{\pm}_{r,s}) > 0$ or $\gamma^{\pm}_{r,s} \geq 0$,

$$(k^{\pm})^2 = \omega^2 \epsilon^{\pm} \mu_0$$

and

$$K_1 = \frac{2\pi}{d_1} \ , \ K_2 = \frac{2\pi}{d_2}.$$

It is clear from (16) that only a finite number of modes propagate away from the grating, since the remaining modes decay exponentially. The main quantities of interest here are the *grating efficiencies*

$$e^{\pm}_{r,s} = \frac{|B^{\pm}_{r,s}|^2 \gamma^{\pm}_{r,s}}{\gamma^{+}_{0,0}} \tag{17}$$

for the finitely many propagating modes, i.e. the modes (r, s) such that $\gamma^{\pm}_{r,s}$ is real.

In this case the principle of conservation of energy can be stated as follows: if we let $U^{\pm}$ denote the set of indices corresponding to the propagating modes in $\Omega^{\pm}$, then

$$\sum_{(r,s)\in U^+} e^{+}_{r,s} + \sum_{(r,s)\in U^-} e^{-}_{r,s} = 1, \tag{18}$$

provided the dielectric constants ϵ^+ and ϵ^- are real.

In the two dimensional case we shall consider gratings of the form

$$\Omega^- = \{x_3 < f(x_1)\}, \tag{19}$$

for which the expansion above reduces to

$$u^{\pm} = \sum_{r=-\infty}^{\infty} B^{\pm}_{r} e^{i\alpha_r x_1 \pm i\gamma^{\pm}_{r} x_3}. \tag{20}$$

The principle of conservation of energy now reads

$$\sum_{r\in U^+} e^{+}_{r} + \sum_{r\in U^-} e^{-}_{r} = 1, \tag{21}$$

where the efficiencies are now given by $e^{\pm}_r = \gamma^{+}_r |B^{\pm}_r|^2 / \gamma^{+}_0$.

3 Analyticity and Taylor coefficients

3.1 Overview

As we said, our algorithms are based on a theorem we established recently [6] of analyticity of the electromagnetic field with respect to boundary variations. To describe our results assume Ω^-_δ is a family of scatterers, one for each value of the real parameter δ —see e.g. Figure 1 and equation (28) below. Further, assume the boundaries Γ_δ of these obstacles admit parametrizations

$$\vec{r} = H(s, \delta) \tag{22}$$

where the function H is jointly analytic in the spatial variable s and the perturbation parameter δ. Our theorems state that both the values $v = v(\vec{r}, \delta)$ of the electromagnetic field at a fixed point in space as well as the values at a point *on the varying boundary* depend analytically on the boundary variations. More precisely, if $\vec{r}$ is a point in space away from Γ_δ and $\vec{r}_\delta \in \Gamma_\delta$ is a point on the interface which varies analytically with δ, then $v(\vec{r}, \delta)$ is jointly analytic in $(\vec{r}, \delta)$, and $v(\vec{r}_\delta, \delta)$ is an analytic function of δ for all real values of δ for which the surface (22) does not self intersect.

It follows from these theorems that the field can be expanded in a series in powers of δ

$$v^{\pm}(\vec{r}, \delta) = \sum_{n=0}^{\infty} v^{\pm}_n(\vec{r}) \delta^n \tag{23}$$

which converges for δ small enough, and that it can be continued analytically to all values of δ for which the surface (22) does not self-intersect. The fields $v^{\pm}_n$ satisfy Maxwell's equations (2) as well conditions of radiation at infinity. They also satisfy boundary conditions on $\Gamma_0 = \Gamma_\delta|_{\delta=0}$ which can be obtained by differentiation as we show below. Such differentiations and use of the chain rule are permissible, as it follows from the analyticity theorems mentioned above and related extension theorems [6]. The explicit solutions v_n lead easily to recursive formulae for the Taylor coefficients of the refracted amplitudes B (see §2.2); together with methods for analytic continuation, this provides a numerical algorithm for the calculation of the scattered field.

Formulae for Taylor coefficients associated with the various kinds of diffraction gratings

$$\Omega_\delta^- = \{x_3 < \delta f(x_1)\} \tag{24}$$

in two dimensions, or

$$\Omega_\delta^- = \{x_3 < \delta f(x_1, x_2)\} \tag{25}$$

in three dimension were given in [7, 8, 9]. In the simplest case of a two dimensional grating (24) in TE polarization, for example, the recursive formula takes the form

$$d_{n,r} = -(-i\beta)^n C_{n,r} - \sum_{k=0}^{n-1} \sum_{q=\max(-kF, r-(n-k)F)}^{\min(kF, r+(n-k)F)} C_{n-k,r-q}(i\beta_q)^{n-k} d_{k,q}\,, \tag{26}$$

$(-nF \le r \le nF)$. Here $d_{n,r}$ are the coefficients in the power series

$$B_r(\delta) = \sum_{k=0}^{\infty} d_{k,r}\delta^k \tag{27}$$

of the amplitudes $B_r(\delta)$ in the eigenfunction expansion of the function $u_1 = E_{x_2}$, see §2.2; and $C_{n,r}$ is the r-th Fourier coefficient of the $f^n/n!$. In the following section we derive recursive formulae for the calculation of the Taylor coefficients of the amplitudes $B_r = B_r(\delta)$ associated with a two dimensional bounded obstacle

$$\Omega^- = \Omega_\delta^- = \{\rho < a + \delta f(\theta)\}; \tag{28}$$

the problem of summation of such series is considered in §5 below. The case of a three dimensional bounded obstacle

$$\Omega_\delta^- = \{\rho < a + \delta f(\theta, \phi)\} \tag{29}$$

will be treated elsewhere.

3.2 Recursive formulae: bounded obstacles in two dimensions

Let us derive formulae for a perfectly conducting and bounded two dimensional object (28) under TE radiation. The interface Γ_δ is given by

$$\Gamma_\delta = \{(\rho, \theta) \,:\, \rho = a + \delta f(\theta)\}\,. \tag{30}$$

(Here we view our obstacle as two dimensional perturbation of a circular cylinder. In some circumstances it may be advantageous to use perturbations from other particular geometries for which exact solutions are known, such as, for example, an appropriate elliptic cylinder or ellipsoid.) In the TE case considered here the transverse component $u = E_{x_2}$ of $\vec{E}$, ($u = u_1$ in the notation of §2), satisfies the Helmholtz equation (4) and the boundary condition

$$u = -e^{i\alpha x_1 - i\gamma x_3} \text{ on } \Gamma_\delta. \tag{31}$$

It is clearly sufficient to consider the case in which the direction of our incident wave is that of the negative x_1-axis, and we thus have

$$\vec{E}^i = \hat{x}_2 e^{-ikx_1}\,, \quad \vec{H}^i = \hat{x}_3\sqrt{\frac{\epsilon^+}{\mu}}e^{-ikx_1}.$$

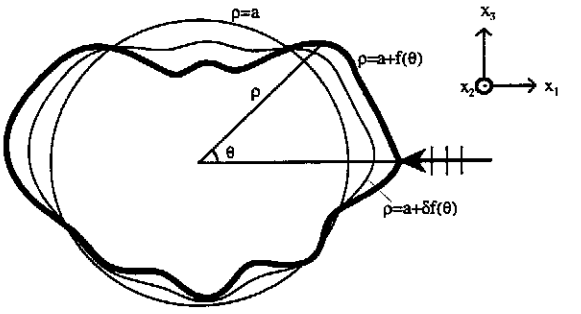

Figure 1: The geometry.

As we said above, our method is based on viewing the scattered fields as functions of the parameter δ and evaluating the corresponding Taylor series expansions. From §3.1 we have an expansion

$$u(\rho, \theta, \delta) = \sum_{n=0}^{\infty} u_n(\rho, \theta)\delta^n$$

which converges for sufficiently small values of δ. The functions

$$u_n(\rho, \theta) = \frac{1}{n!}\frac{\partial^n u}{\partial \delta^n}(\rho, \theta, 0) \tag{32}$$

satisfy the Helmholtz equation

$$\Delta u_n + k^2 u_n = 0 \text{ in } \{\,(\rho, \theta) \,:\, \rho > a\,\}$$

and conditions of radiation at infinity. In view of (11) we see that the functions u and u_n admit expansions of the form

$$u(\rho, \theta, \delta) = \sum_{r=-\infty}^{\infty} B_r(\delta)(-i)^r H_r^{(1)}(k\rho)e^{ir\theta}$$

and

$$u_n(\rho, \theta) = \sum_{r=-\infty}^{\infty} d_{n,r}(-i)^r H_r^{(1)}(k\rho)e^{ir\theta}. \tag{33}$$

We clearly have

$$d_{n,r} = \frac{1}{n!}\frac{d^n B_r}{d\delta^n}(0),$$

so that the amplitudes of the various modes are given by the Taylor series

$$B_r(\delta) = \sum_{n=0}^{\infty} d_{n,r}\delta^n. \tag{34}$$

Our approach proceeds by evaluation of the Taylor series (34), whose coefficients $d_{n,r}$ can be obtained recursively. Such recursive formulae follow from the conditions at the boundary of the obstacle, which in this case may be written in the form

$$u(a+\delta f(\theta),\theta,\delta) = \big|_{\rho=a+\delta f(\theta)} = -e^{-ik(a+\delta f(\theta))\cos(\theta)}. \tag{35}$$

To obtain our recursive relations we first use the well known expansion [18] of the composite function $e^{a\cos(\theta)}$ in terms of exponentials and Bessel functions $J_r(z)$, and we obtain

$$u(a+\delta f(\theta),\theta,\delta) = -\sum_{r=-\infty}^{\infty} (-i)^r J_r\left(k(a+\delta f(\theta))\right) e^{ir\theta}. \tag{36}$$

Differentiation then gives

$$u_n(a,\theta) = -k^n \frac{f(\theta)^n}{n!} \sum_{r=-\infty}^{\infty} (-i)^r \frac{d^n J_r}{dz^n}(ka) e^{ir\theta} - \sum_{l=0}^{n-1} \frac{f(\theta)^{n-l}}{(n-l)!} \frac{\partial^{n-l} u_l}{\partial \rho^{n-l}}(a,\theta). \tag{37}$$

Let now the Fourier series of the function $f(\theta)$ be given by

$$f(\theta) = \sum_{r=-F}^{F} C_{1,r} e^{ir\theta}$$

with either finite or infinite F. Then, substitution in (37) of u_l $(0 \le l \le n)$ and their ρ-derivatives as calculated from (33) permits us to find all the coefficients $d_{n,r}$ in terms of the coefficients $d_{k,r}$ with $k < n$ and the Fourier series coefficients $C_{l,r}$ of the function $f(\theta)^l/l!$:

$$\frac{f(\theta)^l}{l!} = \sum_{r=-lF}^{lF} C_{l,r} e^{ir\theta}.$$

Indeed, from (37) we have

$$\sum_{q=-\infty}^{\infty} d_{n,q}(-i)^q H_q^{(1)}(ka) e^{iq\theta} =$$
$$-k^n \sum_{s=-nF}^{nF} C_{n,s} e^{is\theta} \sum_{r=-\infty}^{\infty} (-i)^r \frac{d^n J_r}{dz^n}(ka) e^{ir\theta}$$
$$-\sum_{l=0}^{n-1} \sum_{s=-(n-l)F}^{(n-l)F} C_{n-l,s} e^{is\theta} \sum_{r=-\infty}^{\infty} d_{l,r}(-i)^r k^{n-l} \frac{d^{n-l} H_r^{(1)}}{dz^{n-l}}(ka) e^{ir\theta}.$$

Collecting terms of like powers of $e^{i\theta}$ in the expression above now yields the desired recursive expression. We obtain

$$d_{n,q} = -k^n \sum_{p=q-nF}^{q+nF} C_{n,q-p}(-i)^{p-q} \frac{d^n J_p}{dz^n}(ka)/H_q^{(1)}(ka)$$
$$-\sum_{l=0}^{n-1} k^{n-l} \sum_{p=q-(n-l)F}^{q+(n-l)F} d_{l,p} C_{n-l,q-p}(-i)^{p-q} \frac{d^{n-l} H_p^{(1)}}{dz^{n-l}}(ka)/H_q^{(1)}(ka). \tag{38}$$

The calculation is initialized by means of the relations

$$d_{0,q} = -J_q(ka)/H_q^{(1)}(ka) \tag{39}$$

which follow from the exact expressions for the field scattered by a circular cylinder of radius a (see [4]).

3.3 Calculation of Taylor coefficients

Recursive formulae such as (26) and (38) allow us to compute Taylor coefficients of a scattering problem to arbitrarily high orders. To demonstrate the calculation, let us consider first the simplest case of the two dimensional grating (24) with

$$f(x_1) = 2\cos(Kx_1) = e^{iKx_1} + e^{-iKx_1}, \tag{40}$$

for which $F = 1$, $C_{n,k} = 0$ if $n-k$ is odd and $C_{n,k} = \frac{1}{n!}\binom{n}{\frac{n-k}{2}}$ if $n-k$ is even. Then, it is easy to see from (26) that the non-zero coefficients $d_{n,r}$ are

$$\begin{array}{ccccccccc} & & & & d_{0,0} & & & & \\ & & & d_{1,-1} & & & d_{1,1} & & \\ & & d_{2,-2} & & d_{2,0} & & d_{2,2} & & \\ & d_{3,-3} & & d_{3,-1} & & d_{3,1} & & d_{3,3} & \\ d_{4,-4} & & d_{4,-2} & & d_{4,0} & & d_{4,2} & & d_{4,4} \\ & & & & etc. & & & & \end{array}$$

If an N-th order approximation to the Taylor series in (27) is to be computed, it is clearly unnecessary to produce *all* of the coefficients $d_{n,r}$ for $n \le N$. In fact, to compute B_0 with $N = 4$ we need only generate

$$\begin{array}{ccccc} & & d_{0,0} & & \\ & d_{1,-1} & & d_{1,1} & \\ d_{2,-2} & & d_{2,0} & & d_{2,2} \\ & d_{3,-1} & & d_{3,1} & \\ & & d_{4,0} & & \end{array} \tag{41}$$

Of course, in general we wish to obtain not only B_0 but a number of amplitudes B_r, $|r| \le w$, which will be in turn used to calculate the fields with a given accuracy, and the arrays of derivatives must be augmented accordingly. Similar considerations apply to functions f given by an arbitrary finite Fourier series.

In practice, and in order to reduce the number of operations, one can choose to truncate the inner sum in equations such as (26) by setting $d_{k,q} = 0$ for $|q| > q_0$. The parameter q_0 has to be chosen judiciously. Our experiments indicate that in the case of the sinusoidal profile (40), no truncation is permissible (e.g. one cannot take $q_0 < 2$ in (41)). On the other hand, for the grating associated with the function

$$f(x_1) = 2\cos(Kx_1) + \frac{1}{5}\cos(3Kx_1), \qquad (42)$$

for example, the effect of the higher order harmonics generated by the second summand can be truncated. In other words, even though the actual formula (26) for this profile involves frequencies roughly as high as $\frac{3}{2}N + w$, one can take $q_0 = \frac{N}{2} + w$ with errors comparable to roundoff. This is related to the fact that the height-to-period ratio h/d of the first term in (42) is larger than the one for the second term. Thus, in the general case of a general Fourier series q_0 should be chosen so that no truncation would occur if all but the principal terms in it (i.e. the ones with the largest h/d's) were neglected. Naturally, as the height-to-period ratio of a secondary term approaches the ones for the principal terms, the value of q_0 should be increased. The ultimate choice of q_0 must be made by consideration of the actual errors as measured by the defect in the energy balance, convergence, reciprocity or other criteria.

In the case of the sinusoidal grating considered above, closed form expressions for the coefficients $C_{n,r}$ occurring in equation (26) were found. (Again, $C_{n,r}$ is the r-th Fourier coefficient of the $f^n/n!$). Of course, it is not possible to obtain such closed form expressions for the C coefficients in case the boundary of the scatterer is given by an arbitrary function f. By appropriate truncation we may always assume f equals a *finite* Fourier series containing modes with orders between $-F$ and F, say; simple iterated multiplication of the series of f then yields a very stable algoritm for the calculation of $C_{n,r}$. Convergence of the calculated scattered field as F is increased is then the criterion for an appropriate choice of this parameter.

Now, calculation of complete powers f^n in the three dimensional cases may be prohibitively expensive —even when F is as small as, say, $F = 10$. It is therefore fortunate that, again, appropriate truncations can be used with errors comparable with roundoff. The procedure is very simple indeed: if the Fourier series of f^n has been computed, then all modes of order r with $|r| > q_1$ are set to zero, and the resulting series is multiplied by the series of f. The result is then taken as an approximation to f^{n+1}. Of course, the choice of the parameter q_1 depends on the particular scatterer, on F, on q_0, and on the order n of the Taylor approximation. We can assume appropriate values of these parameters have been found when further increases in them do not lead to improvements in the numerical error.

To complete our algorithms we must now consider the question of summation of Taylor series such as (27). As we have said, the functions $B_r(\delta)$ are analytic in a common neighborhood of the real axis and therefore, the series in (27) certainly has a positive radius of convergence. It turns out that this series diverges (or converges slowly) for many cases of interest, and we thus need appropriate numerical schemes for analytic continuation in the complex δ plane. This is the subject of the following section.

4 Approximation of analytic functions

Our understanding of the problem of calculation of the electromagnetic field by means of analytic continuation can be presented at two different levels of detail. On one hand we may accurately state that Padé approximants have produced better accuracy than other approximators in all the applications of our method we have encountered. We therefore view Padé approximation, which is briefly described below, as an integral element of our algorithms. An interesting insight in the approximation problem, on the other hand, can be gained by consideration of the spectrum of singularities of the field *as a function of the perturbation parameter* δ. Indeed, singularities play a major role in the approximation problem. They determine the radius of convergence of the Taylor series and they are closely related to the speed of convergence of Padé approximants [1]. Further, the spectrum of singularities determines the conditioning in the values of the Padé approximants [10], and even partial information on such singularities may be used in some cases to produce a rather dramatic improvement in the Padé problem: a simple example of this phenomenon is presented at the end of this section. Padé approximants and the analytic structure of the field in the δ plane are discussed in what follows.

The $[L/M]$ Padé approximant of a function

$$B(\delta) = \sum_{n=0}^{\infty} d_n \delta^n \qquad (43)$$

is defined (see [1]) as a rational function

$$[L/M] = \frac{a_0 + a_1\delta + \cdots + a_L\delta^L}{1 + b_1\delta + \cdots + b_M\delta^M}$$

whose Taylor series agrees with that of B up to order $L+M+1$.

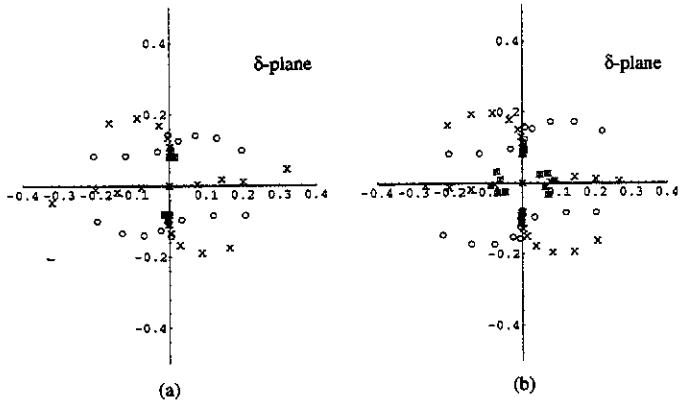

Figure 2: Poles (o) and zeros (x) of the Padé approximants of $B_1(\delta)$: (a) [28/28]-approximant and (b) [48/48]-approximant.

A particular $[L/M]$ approximant may fail to exist but, generically, $[L/M]$ Padé approximants exist and are uniquely determined by L, M and the first $L+M+1$ coefficients of the Taylor series of B. Padé approximants have some remarkable properties of approximation of analytic functions from their Taylor series (43) for points far outside their radii of convergence, see e.g. [1]. They can be calculated by first solving a set of linear equations for the denominator coefficients b_i, and then using simple formulae to compute the numerator coefficients a_i. For convergence studies and numerical calculation of Padé approximants see [1, 2, 5, 15].

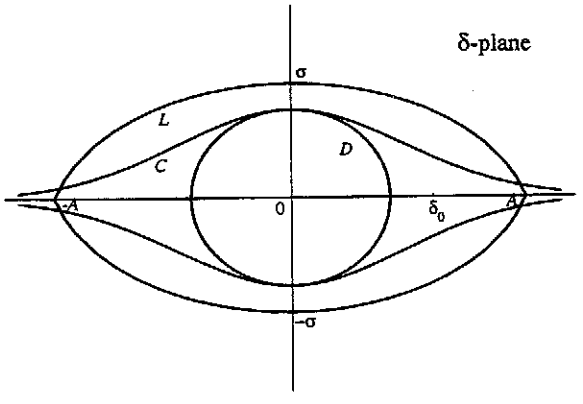

Figure 3: The region C of analyticity of the Rayleigh coefficients $B_r^{\pm}(\delta)$ and a lens-shaped region L that is conformally transformed onto the right-half plane via $g(\delta) = (\frac{A-\delta}{A+\delta})^{\alpha}$.

In Figure 2 we show the location of the zeroes of the numerators and denominators of the [28/28] and [48/48] Padé approximants to the coefficient $B_1(\delta)$ for the perfectly conducting grating with profile

$$f_\delta(x_1) = \delta(e^{i2\pi x_1} + e^{-i2\pi x_1}) = 2\delta\cos(2\pi x_1)$$

under normal incidence and with light of wavelength $\lambda = 0.4368$. In this figure, a circle ('o') represents a zero of the denominator, which is a singularity of the approximant provided it is not crossed out by a corresponding zero ('x') in the numerator. Very similar pictures are obtained for other amplitudes B_r and for approximants of other orders. Now, it is well known that, rather generally, the singularities of the Padé approximants approach the singularities of the function they approximate [1]. Thus, Figure 2 provides us with an approximation to the domain of analyticity of the diffracted fields. Note that no singularities occur on the real axis, as expected from the theoretical discussion of §3.1.

A domain of analyticity C which is consistent with the one suggested by Figure 2 was proposed in [7], see Figure 3. This picture lead us to devise a summation mechanism based on conformal transformations which we called *enhanced convergence* [6, 10], see also [32]. Given a function $B(\delta)$ and a complex number δ_0, the method of enhanced convergence uses conformal mappings to produce an appropriate arrangement of the singularities of B and the point δ_0, so that a truncated Taylor series can be used to calculate $B(\delta_0)$.

To describe this method, let us suppose we wish to compute the function $B(\delta)$ at a point δ_0 which lies outside the circle of convergence D of the Taylor series of B around $\delta = 0$ (see Figure 3). The series is divergent at δ_0. If we consider, however, the composition of B with a conformal transformation,

$$\xi = g(\delta),$$

the singularities and the point $\xi_0 = g(\delta_0)$ at which the function is sought will show a different arrangement *in the ξ-plane* and, possibly, ξ_0 will lie inside the circle of convergence of the composite function $B(g^{-1}(\xi))$. If so, a truncated Taylor series of the composite function can be summed to yield the value $B(\delta_0)$. Even if δ_0 lies inside the circle of convergence D, this procedure may result in improved convergence rates [7, 10]. In Tables 1 and 2, for example, we compare the convergence of the power series for $e_1(\delta) = |B_1(\delta)|^2\beta_1/\beta_0$ about $\delta = 0$ ("Direct") with that of $e_1(\xi) = |B_1(\xi)|^2\beta_1/\beta_0$ ("Enhanced") obtained by means of an appropriate conformal change of variables [6]. Again we consider the sinusoidal grating scattering problem mentioned above. We observe that even in the case $\delta = 0.075$, in which the direct series converges, the convergence is substantially enhanced by

the conformal mapping. In case $\delta = 0.1$ the direct series does not converge.

	Direct		Enhanced	
n	e_1	ϵ	e_1	ϵ
10	0.5034545E–02	1.5E–01	0.1735547E–01	8.3E–02
15	0.1073396E–01	5.3E–02	0.1204894E–01	1.3E–05
20	0.1045474E–01	4.0E–03	0.1157684E–01	5.1E–04
25	0.1140532E–01	3.2E–03	0.1163189E–01	3.1E–05
30	0.1161950E–01	2.2E–04	0.1163870E–01	–8.4E–06
35	0.1165000E–01	1.1E–05	0.1163798E–01	–7.3E–07
40	0.1162548E–01	–3.2E–05	0.1163793E–01	–4.4E–08
45	0.1163059E–01	5.1E–05	0.1163793E–01	2.2E–08
50	0.1164204E–01	1.2E–05	0.1163793E–01	2.0E–09
55	0.1164090E–01	–1.7E–05	0.1163793E–01	–3.7E–11
60	0.1163616E–01	–4.0E–06	0.1163793E–01	–4.5E–11

Table 1: Comparison between direct and enhanced convergence. First order efficiency for a sinusoidal grating in TE polarization, $\delta = 0.075$.

	Direct		Enhanced	
n	e_1	ϵ	e_1	ϵ
10	0.3897061E+00	–7.2E–01	0.4018525E+00	–4.5E–01
15	0.4713435E+01	–1.4E+01	0.1649737E+00	–7.3E–02
20	0.3635994E+01	–1.5E+01	0.1568326E+00	3.1E–02
25	0.3848452E+01	–1.2E+01	0.1687898E+00	4.8E–03
30	0.3357765E+00	–5.5E+00	0.1698172E+00	3.0E–04
35	0.1276039E+01	–2.4E+01	0.1701259E+00	–4.0E–04
40	0.4143993E+02	–2.2E+02	0.1700261E+00	–1.3E–04
45	0.1665033E+03	–1.6E+03	0.1699795E+00	1.3E–05
50	0.1406855E+04	–8.2E+03	0.1699760E+00	1.1E–05
55	0.7075471E+04	–6.9E+04	0.1699781E+00	2.5E–06
60	0.7847034E+05	–4.1E+05	0.1699792E+00	–4.8E–07

Table 2: Comparison between direct and enhanced convergence. First order efficiency for a sinusoidal grating in TE polarization, $\delta = 0.1$.

The performance of this summation method depends strongly on the parameters A and σ of Figure 3. The optimality of a choice of these parameters can be checked through the defect ϵ in the energy relation (21)

$$\epsilon = 1 - \sum_{n \in U^+} e_n^+.$$

($e_n^- = 0$ here, since we are dealing with a perfectly conducting grating.) Alternatively, the optimal values of these parameters can be calculated [8] by consideration of the poles shown in Figure 2. The results of these two calculations for A and σ are in close agreement. Further, note the position of singularities closest to the origin in Figure 2, which imply a radius of convergence consistent with the convergence results of the direct series in Tables 1 and 2. The agreements found in these calculations constitute an important consistency check in our theory. They add substantial credibility to our view that the analytic structure in the δ plane is well approximated by representations such as that in Figure 2.

As we said, Padé approximation does exhibit better numerical performance than enhanced convergence; in the examples of Table 1 and 2, for instance, Padé approximants permit us to obtain two additional significant digits [8]. Interestingly, enhanced convergence can be used to improve the performance of Padé approximation. Indeed, the theory in [10] shows that the relative arrangement of the singularities of an analytic function is closely related to the numerical conditioning of the corresponding Padé problem. Further, a conformal change of variables on a function $B(\delta)$ can lead to a dramatic improvement in this conditioning. (The Padé approximants of the functions in the transformed variables will be referred to as enhanced Padé approximants.) Since the main numerical weakness of Padé approximation is its ill conditioning, it is reasonable to expect that enhance approximants could lead to improvement in our solutions of scattering problems.

Whether or not this is the case remains an issue for further investigation, since there is a requisite that needs to be met: accurate values of the Taylor coefficients of the composite functions must be used. Composition of the corresponding series, which certainly suffices in applications such as those of Tables 1 and 2, is not appropriate for the enhanced Padé application. Indeed, composition of power series leads to a loss of significant digits in the Taylor coefficients. This accuracy loss interacts with the conditioning problem of Padé approximation in such a way that no substantial improvements in the calculated values are obtained. If accurate values of the coefficients of the composite functions can be found, on the other hand, then very substantial improvements can be obtained as shown in an example below. Thus, further improvement in the performance of our algorithms could result if an accurate method for computation of the enhanced coefficients were found.

As we said, enhanced convergence may help obtain a remarkable improvement in the performance of Padé approximation. To illustrate this point we consider Table 3 below, which shows the values of the $[\frac{N}{2}/\frac{N}{2}]$ Padé and Enhanced Padé approximants for the function $f(z) = \log(1+z)$, see [10] for details. This Table shows that enhanced Padé approximants produce up to 13 correct digits of log(21) while ordinary Padé fractions do not produce more than the first four digits. Table 3 also shows the values of both approximants at $z = 200$; again an improvement is observed.

N	z	$\log(1+z)$	Padé	Enh. Padé
20	20	3.044522437723	3.043989111079	3.043988784141
40			3.044612164211	3.044522360574
60			3.044477040660	3.044522437596
80			3.044175772366	3.044522437727
100			3.044463021924	3.044522437722
120			3.044489520809	3.044522437724
140			3.044496462919	3.044522437723
160			3.044619592662	3.044522437723
180			3.044362344599	3.044522437723
20	200	5.30330	5.03582	5.03577
40			5.32614	5.28588
60			5.17831	5.30093
80			5.08690	5.30276
100			5.16939	5.30305
120			5.18899	5.30324
140			5.19792	5.30328
160			5.70660	5.30329
180			5.13885	5.30330

Table 3: $[\frac{N}{2}/\frac{N}{2}]$ approximants for $\log(1+z)$

5 Applications

The difficulty associated with the numerical solution of a scattering problem depends roughly on two elements: the ratio P/λ of the size of the scatterer to the wavelength on one hand, and the oscillations and/or lack of smoothness exhibited by its boundary, on the other. In short, numerical complexity arises from the need to account accurately for oscillatory behavior of fields and interfaces. In what follows we present applications of our method which test its performance in problems of various degrees of complexity, and we compare the results of our algorithms with those given by classical methods.

As we have noted, our approach is applicable to configurations which may be viewed as perturbations from an exactly solvable geometry. Such perturbations need not be small —as it may be seen from the examples that follow—, and our analytic method may be considered as a rather general one. In many cases of practical importance our approach yields results that are several orders of magnitude more accurate than those given by classical methods —such as the method of moments and other algorithms based on the solution of integral equations.

5.1 Two dimensional problems

We have tested our analytic method in a variety of problems of diffraction by gratings and bounded obstacles. Our method was originally intended as a grating solver; we therefore discuss applications to grating problems first. In the following sections the error estimator ϵ is the defect in the energy balance criterion. For example, in the grating configurations ϵ is defined as the defect in the relations (18) and (21), e.g., for two dimensional dielectric gratings ϵ is given by

$$\epsilon = 1 - \sum_{r\in U+} e_r^+ - \sum_{r\in U-} e_r^-$$

as calculated by the numerical solver. For a perfectly conducting bounded obstacle in two dimensions ϵ is defined as the relative error in the calculated value of the left hand side in equation (12)

$$\epsilon = \frac{\left|\sum_r |B_r|^2 + \mathrm{Re}\left(\sum_r B_r\right)\right|}{\sum_r |B_r|^2}. \tag{44}$$

These defects provide an accurate measure of the relative error in most quantities of interest. This is quite clear in the grating applications, in which the efficiencies themselves are the quantities sought. In the bounded obstacle problem, on the other hand, ϵ is closely related to the relative error in the numerical value of the forward scattering. Of course, the energy balance criterion is only valid in the absence of absorption; when dealing with lossy scatterers we generally turn to estimating the errors by means of convergence tests (see e.g. the first application in §5.2). Further, ϵ only estimates errors in far field quantities; for near fields errors one would need to turn, again, to convergence tables.

In our first example we consider a problem of diffraction by a sinusoidal dielectric grating (24) with

$$f(x_1) = 2\cos(2\pi x_1/d) \tag{45}$$

and period $d = 1\mu m$. (Note that the height h of the corrugations —that is, the vertical distance from the highest peak to the lowest valley— is given by $h = 4\delta$.) The grating has a refractive index $\nu_0 = 2$, and is illuminated under normal incidence with light of wavelength $\lambda = 0.83\mu m$. Table 4 contains results given by our algorithms for the reflected and transmitted energy R and T which results from a unit input energy. This case was treated in [13] by means of integral equations and the method of moments; there the authors report the following values of R and T for $h = 0.2\mu m$:

$$R = 0.117274,$$

$$T = 0.882759$$

and

$$\epsilon = 1 - (T + R) = 3.3 \times 10^{-5};$$

compare Table 4a.

	(a)			(b)		
h/d	R	T	ϵ	R	T	ϵ
0.00	0.111111	0.888889	-2E-16	0.111111	0.888889	-2E-16
0.10	0.114926	0.885074	0E00	0.104046	0.895954	-2E-16
0.20	0.117282	0.882718	0E00	0.086355	0.913645	0E00
0.30	0.104871	0.895129	1E-14	0.062807	0.937193	-1E-12
0.40	0.080184	0.919816	9E-11	0.039117	0.960883	-1E-08
0.50	0.055902	0.944098	1E-07	0.025636	0.974363	-6E-07
0.60	0.038983	0.961015	-1E-06	0.023655	0.976517	1E-04
0.70	0.029619	0.969848	-5E-04	0.021333	0.982000	3E-03
0.80	0.024083	0.972233	-3E-03	0.016013	0.999951	1E-02

Table 4: Reflected and transmitted energies for a sinusoidal grating with index of refraction $\nu_0 = 2$, under normal incidence with a wavelength-to-period ratio $\lambda/d = 0.83$: [20/20] Padé approximants. Table 4a.: TE polarization; Table 4b.: TM polarization.

As it is the case here, the analytic method yields results of very good definition in most grating problems of interest. Other results for grating problems obtained by discretization of boundary integral equations include, for example, those of Van Den Berg [35] and Pavageau and Bousquet [27]. These authors considered a perfectly conducting sinusoidal grating for values of h/d ranging from 0.3 to 0.56 and illuminated with light of wavenlength $\lambda = 0.4368$. They report errors of the order of 10^{-5} for a ratio of 0.3 and of order 10^{-3} for ratios of 0.4 and .56. The corresponding errors in the analytic method are of order 10^{-12}, 10^{-8} and 10^{-6}; similar improvements in performance over other methods has been found in calculations containing lossy gratings and nonsmooth (e.g. triangular) profiles [8]. It must be pointed out that the largest ratio $h/d = 0.56$ considered here is larger than those corresponding to gratings actually used in applications [24]. For even deeper gratings, say ratios of 0.7 and beyond (and for this wavelength), our method in its present form rapidly breaks down due to numerical ill conditioning, while the integral method deteriorates more slowly, and it gives results with errors of a few percent for gratings with heights as large as $h/d = 1$. As we pointed out in §4, remedies for conditioning problems in our algorithms may result from a more detailed consideration of the analytic properties and singularities of the electromagnetic field, see e.g. Table 3.

In our second example we study the scattering by the perfectly conducting obstacle of Figure 4 (a): a two-dimensional bounded scatterer without symmetries. The boundary of this obstacle is given by (30) with $f(\theta) = 0.125\sin(4\theta) - 0.15\sin(3\theta)$ and $\delta = 1$. Figure 4 (b) gives the amplitude of the bistatic far field coefficient Φ for the TE polarized configuration indicated in Figure 4 (a) with perimeter-to-wavelength ratio $P/\lambda = 20$.

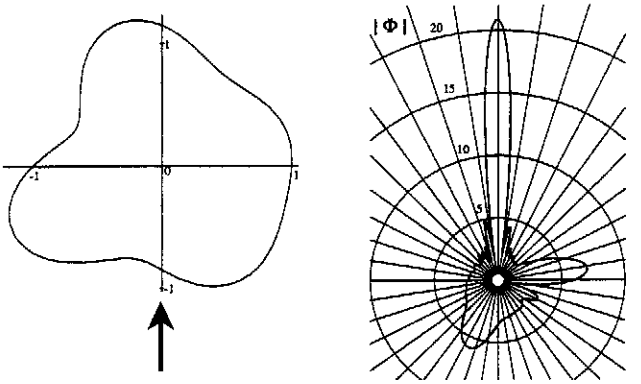

(a) (b)

Figure 4: (a) a two dimensional bounded scattering configuration without symmetries and (b) the amplitude of its bistatic far field coefficient Φ. TE polarization, $P/\lambda = 20$.

In order to test the ability of our algorithms to compute the scattering by large objects and by objects with pronounced protuberances we present calculations corresponding to the scatterers of Figures 5 and 6. The boundaries of these obstacles are again given by (30), this time with

$$f(\theta) = 2\cos(4\theta),$$

see equation (28), and the values $\delta = 0.15/4$ and $\delta = 0.75/4$. In Tables 5 and 6 we give the back-scattering cross section (BSCS), forward scattering cross section (FSCS) and total scattered energy ($\sum_r |B_r|^2$) corresponding to these bodies for a variety of perimeter to wavelength ratios P/λ.

P/λ	BSCS	FSCS	Energy	ϵ
20	1.609e+00	1.006e+02	2.210e+01	3e–16
40	1.599e+00	1.930e+02	4.339e+01	1e–15
60	1.597e+00	2.851e+02	6.463e+01	5e–14
80	1.597e+00	3.768e+02	8.582e+01	4e–13
100	1.596e+00	4.684e+02	1.070e+02	2e–10

Table 5: Computed values of the back-scattering cross section (BSCS), forward scattering cross section (FSCS) and total scattered energy ($\sum_r |B_r|^2$) for the scatterer of Figure 5: [29/29] Padé approximants. ($w = 150$; $q_0 = 180$).

Consider first Table 5 which corresponds to the scatterer of Figure 5. (Here, as well as in Table 6, q_0 and w are the truncation and mode parameters defined in § 3.3.) Note that excellent accuracy obtained in this case for wavelengths as small as $\frac{1}{100}P$. We have been unable to find detailed estimates of the errors produced

by other methods for problems of this type. Consideration of solutions available in the literature in forms of graphs does suggest that, for configurations like the ones we treat here, the analytic method can make a rather competitive solver.

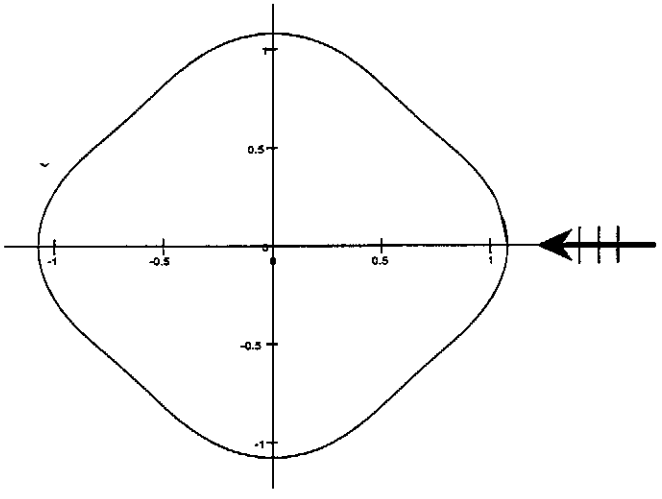

Figure 5: The domain $\Omega_\delta = \{(\rho,\theta) : \rho \leq a + \delta f(\theta)\}$ for $a = 1.0$, $\delta = .15/4$ and $f(\theta) = 2\cos(4\theta)$.

Finally, in Table 6 we give numerical results corresponding to the cross shaped scatterer of Figure 6, which constitutes a much more dramatic perturbation of the circle ($4\delta = 0.75$). The results of Table 6 show that, even for such a complex large scatterer, our solver produces rather accurate results for a wide range of perimeter-to-wavelength ratios.

P/λ	BSCS	FSCS	Energy	ϵ
5	4.448e+00	2.868e+01	4.911e+00	5e–09
10	6.453e+00	6.072e+01	1.024e+01	6e–08
15	7.691e+00	8.916e+01	1.519e+01	2e–06
20	7.984e+00	1.128e+02	1.974e+01	4e–05
25	7.338e+00	1.388e+02	2.453e+01	2e–04

Table 6: Computed values of the back-scattering cross section (BSCS), forward scattering cross section (FSCS) and total scattered energy ($\sum_\tau |B_\tau|^2$) for the scatterer of Figure 6: [29/29] Padé approximants. ($w = 70$; $q_0 = 120$).

5.2 Three dimensional problems

Previous applications of our method in problems of scattering by three dimensional gratings were restricted to sinusoidal surfaces due, in part, to the large number of arithmetic operations involved in a complete calculation of the Taylor coefficient for large values of F. The obvious first step towards extending our method to other significant three dimensional problems, including those involving bounded obstacles, is to tackle the problem of a general biperiodic corrugated surface. To test our method in a challenging case we took a scattering surface with a slowly convergent Fourier series. The results of our work in this direction are discussed below. Our first 3-d example, however, is that of the sinusoidal biperiodic grating first treated in [25].

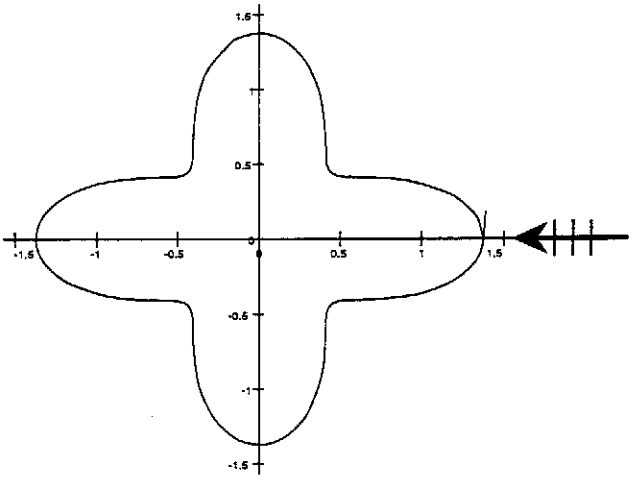

Figure 6: The domain $\Omega_\delta = \{(\rho,\theta) : \rho \leq a + \delta f(\theta)\}$ for $a = 1.0$, $\delta = .75/4$ and $f(\theta) = 2\cos(4\theta)$.

Bisinusoidal gratings in gold have been used in the experimental and numerical studies on total absorption, see [25]. These are gratings of the form (25) with

$$f(x_1, x_2) = \left[\cos\left(\frac{2\pi x_1}{d_1}\right) + \cos\left(\frac{2\pi x_2}{d_2}\right)\right]; \qquad (46)$$

note that the groove depth is again given by $h = 4\delta$. These surfaces (with $h = 0.040$, $h = 0.055$ and $h = 0.070$, and $d_1 = d_2$) were treated in [25] by means of the integral method of [12]. In Figure 8, where we have denoted $d = d_1 = d_2$, we show the results given by our algorithm for this problem. Qualitative agreement with the results in [12, 25] is observed, but some discrepancies occur. For example, in contrast with Figure 7.17 of [25], our curves 2 and 3 coincide at $d = 0.62\mu$m. This prompted us to analyze the accuracy of our results. We found that, for this range of parameters, our method yields extremely accurate results, with errors in the reflected energy ("E. R.") which are better than 10^{-14}. This can be seen in Table 7, which contains a convergence study for the values of the reflected energy at $d = 0.62\mu m$ for the curves labeled 2 and 3 in Figure 8. Note that an accuracy better than 8 digits is obtained by an approximation of order 13. The accuracy of the integral method in this problem ($h = 0.055$

and $h = 0.070$) has been estimated to be of the order of two digits [12]. To demonstrate the range of parameters in which our method can be applied, we include a third column in Table 7 showing the values of E. R. for a much deeper grating profile of height $h = 0.500\mu$m, for which $h/d = 0.806$. We see that even in this case, the results are quite accurate: the errors are of the order of 10^{-4} for a [6/6] approximant ($n = 13$) and of 10^{-6} for a [14/14] approximant ($n = 29$) (Padé approximants with n=15, 19, 23, 27 and 31 are singular for this problem.) The computing time used for the calculation of the Taylor coefficients and the corresponding Padé approximants with $n = 13$ was of about twenty seconds in a Sparc station IPX. We find the results in the first row of Table 7 rather satisfactory, and even more so taking into account the limited computer power they required.

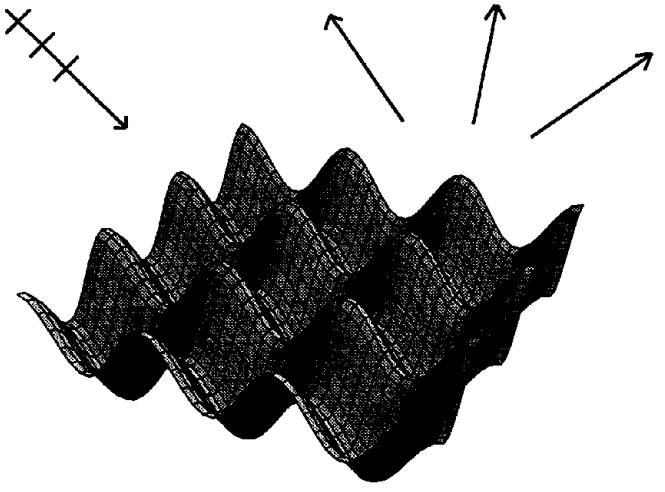

Figure 7: Section of a three dimensional bisinusoidal diffraction grating.

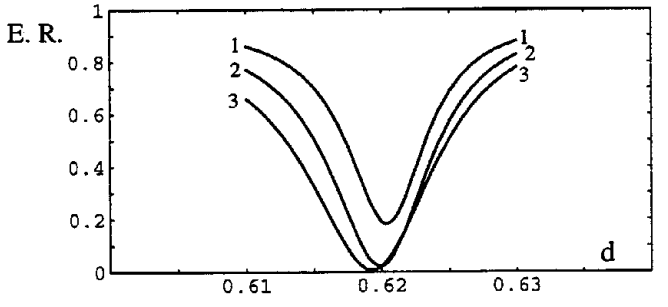

Figure 8: Energy reflected by the bisinusoidal grating of Figure 7 (in gold), with normally incident light of wavelength 0.65μm. 1. $h = 0.040\mu$m; 2. $h = 0.055\mu$m; 3. $h = 0.070\mu$m: [6/6] Padé approximant.

n	$h = 0.055\mu m$	$h = 0.070\mu m$	$h = 0.500\mu m$
13	0.0227882361359963	0.02260573614310	0.84146746
17	0.0227882361334883	0.02260573598742	0.84202623
21	0.0227882361334891	0.02260573598748	0.84219841
25	0.0227882361334900	0.02260573598746	0.84260919
29	0.0227882361334896	0.02260573598742	0.84197301
33	0.0227882361334896	0.02260573598742	0.84197398

Table 7: Convergence study of the reflected energy for the example in Figure 7 (gold). The period is fixed at 0.62μm and the wavelength at 0.65μm. $[\frac{n-1}{2}/\frac{n-1}{2}]$ Padé approximants.

Finally, let us consider the problem proposed in [12], that is, a crossed grating of rectangular pyramids with periods $d_1 = 1.50$ and $d_2 = 1$, of height $h = 0.25$, under incident light of wavelenght $\lambda = 1.533$ and with incidence angles given as follows: cylindrical angle $\phi = 45°$; azimuthal angle $\theta = 30°$ and polarization with the electric field in the vertical plane $\phi = 45°$. This is an interesting configuration, which contains a three dimensional obstacle with corners and edges. A schematic representation of the grating is given in Figure 9. As we have said, our algorithm requires the boundary of the scatterer to be approximated by a finite Fourier series, thus effectively rounding its edges. For comparison purposes we show, in Figure 10, one element of the grating of Figure 9 together its Fourier series approximation with $F = 10$. We can conclude we have obtained the exact solution for the actual pyramid grating within a given error tolerance when convergence within that tolerance is observed as the number of Fourier modes in the approximation is increased.

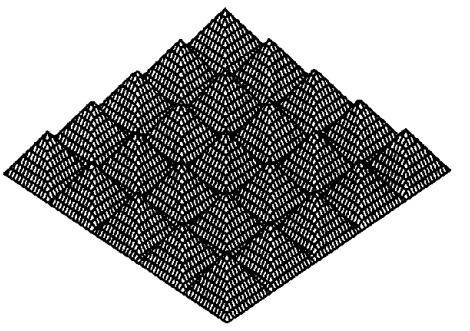

Figure 9: A three dimensional array of square pyramids.

As we explained in §3.3, it is necessary here to choose appropriately the truncation parameters F, q_0 and q_1 as well as the order n of the approximation. In the cases below we found that convergence to the actual numerical solution within the error estimates indicated in Table 8(a) is achieved with $F = 5$, $q_0 = q_1 = 20$ and $n = 9$. Indeed, additional calculations with $F = 10$ and with

$q_0 = q_1 = 22$, 24 and 30 result in no changes in the values of Table 8(a) —exception being made for small changes in the error estimator. This suggests that the solution obtained with $F = 5$ is, within the accuracy shown in Table 8(a), the exact solution to the sharp-edge problem under consideration. These results were produced by a 90 second calculation on a Sparcstation 20.

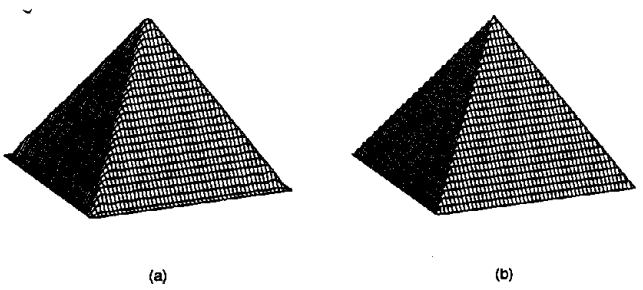

Figure 10: An element of the grating of Figure 9 (a) Fourier approximation with $F = 10$; (b) exact.

An integral algorithm was applied to this problem in [12]; the results reported in that paper are listed in Table 8(b). In addition to results given by the integral method, which is the one the authors recommend, they also presented calculations performed by means of two other solvers based on solution of ordinary differential equations. These differential methods are known to be unstable and generally less competitive than those based on solutions of integral equations [36]. Interestingly, in this particular case one of the differential algorithms produced good results with defect ϵ of order $2 \cdot 10^{-5}$; the other produced $2 \cdot 10^{-3}$.

	(a)			(b)
	$h = 0.05$	0.25	0.50	0.25 (ref. [12])
$e_{r,0,0}$	0.02500	0.01951	0.00858	0.01984
$e_{r,-1,0}$	0.00010	0.00246	0.00713	0.00254
$e_{t,0,0}$	0.97432	0.96465	0.93933	0.96219
$e_{t,1,0}$	0.00012	0.00280	0.00885	0.00299
$e_{t,-1,0}$	0.00013	0.00294	0.01070	0.00303
$e_{t,0,-1}$	0.00029	0.00679	0.02241	0.00704
$e_{t,-1,-1}$	0.00004	.00086	0.00278	0.00092
ϵ	-2E-12	-1E-06	-2E-04	1E-03

Table 8: Efficiencies for the grating of pyramids described in the text. First three columns of results: [4/4] Padé approximants. Last column: values given in reference [12].

Acknowledgements: OB gratefully acknowledges support from NSF (through an NYI award and through grants No. DMS-9200002 and DMS-9523292), from the Sloan Foundation (through the fellowships program) and from the Powell Research Foundation. FR gratefully acknowledges support from AFOSR through grant No. F49620-95-1-0113.

References

[1] G. A. Baker and P. Graves–Morris, *Padé Approximants. Part I: Basic Theory*, Addison–Wesley, Massachusetts, 1981.

[2] G. A. Baker and P. Graves–Morris, *Padé Approximants. Part II: Extensions and Applications*, Addison–Wesley, Massachusetts, 1981.

[3] A. Bayliss and E. Turkel, "Radiation boundary conditions for wave-like equations," Comm. Pure Appl. Math. **33** (1980), 707–725.

[4] J. J. Bowman, T. B. A. Senior and P. L. E. Uslenghi, *Electromagnetic and acoustic scattering by simple shapes*, Revised Printing, Hemisphere Publishing Co., New York, 1987.

[5] C. Brezinski, "Procedures for estimating the error in Padé approximation," Math. Comp. **53** (1965), 639–648.

[6] O. P. Bruno and F. Reitich, "Solution of a boundary value problem for Helmholtz equation via variation of the boundary into the complex domain," Proc. Roy. Soc. Edinburgh **122A** (1992), 317–340.

[7] O. P. Bruno and F. Reitich, "Numerical solution of diffraction problems: a method of variation of boundaries," J. Opt. Soc. Amer. A **10** (1993), 1168–1175.

[8] O. P. Bruno and F. Reitich, "Numerical solution of diffraction problems: a method of variation of boundaries II. Dielectric gratings, Padé approximants and singularities," J. Opt. Soc. Amer. A **10** (1993), 2307–2316.

[9] O. P. Bruno and F. Reitich, "Numerical solution of diffraction problems: a method of variation of boundaries III. Doubly periodic gratings," J. Opt. Soc. Amer. A **10** (1993), 2551–2562.

[10] O. P. Bruno and F. Reitich, "Approximation of analytic functions: a method of enhanced convergence," Math. Comp. **63** (1994), 195–213.

[11] M. G. Cote, M. B. Woodworth and A. D. Yaghjian, "Scattering from the perfectly conducting cube," IEEE Trans. Antennas Propagat. **36** (1988), 1321–1329.

[12] G. H. Derrick, R. C. McPhedran, D. Maystre and M. Nevière, "Crossed gratings: a theory and its applications," in *Electromagnetic Theory of Gratings*, R. Petit ed., Springer, Berlin (1980), 227–275.

[13] D. C. Dobson, and J. A. Cox, "An integral equation method for biperiodic diffraction structures," in *Proceedings of the International Society for Optical Engineering* (SPIE) **1545** (1991), 106–113.

[14] B. Engquist and A. Majda, "Absorbing boundary conditions for the numerical simulation of waves," Math. Comp. **31** (1977), 629–651.

[15] P. Graves–Morris, "The numerical calculation of Padé approximants," in *Lecture Notes in Mathematics* **765**, L. Wuytack ed., Springer, Berlin (1979), 231–245.

[16] J. J. Greffet and Z. Maassarani, "Scattering of electromagnetic waves by a grating: a numerical evaluation of the iterative series solution," J. Opt. Soc. Am. A **7** (1990), 1483–1493.

[17] R. F. Harrington, *Field computation by moment methods*, IEEE Press Series on Electromagnetic Waves, 1993.

[18] D. S. Jones, *The theory of electromagnetism*, The McMillan Co., New York, 1964.

[19] A. Khebir and J. D'Angelo, "A new finite element formulation for RF scattering," IEEE Trans. Antennas Propag. **41** (1993), 534–541.

[20] C. Lopez, F. J. Yndurain and N. García, "Iterative series for calculating the scattering of waves from a hard corrugated series," Phys. Rev. B. **18** (1978), 970–972.

[21] D. Maystre, "Rigorous vector theories of diffraction gratings," in *Progress in Optics*, E. Wolf ed., North Holland, Amsterdam (1984), 3–67.

[22] D. Maystre, "Integral Methods," in *Electromagnetic Theory of Gratings*, R. Petit ed., Springer, Berlin (1980), 63–100.

[23] D. Maystre, and M. Nevière, "Electromagnetic theory of crossed gratings," J. Optics **9** (1978), 301–306.

[24] D. Maystre, M. Nevière, and R. Petit, "Experimental verifications and applications of the theory," in *Electromagnetic Theory of Gratings*, R. Petit ed., Springer, Berlin (1980), 159–223.

[25] R. C. McPhedran, G. H. Derrick, and L. C. Botten, "Theory of crossed gratings," in *Electromagnetic Theory of Gratings*, R. Petit ed. Springer, Berlin (1980), 227–275.

[26] W. C. Meecham, "On the use of the Kirchoff approximation for the solution of reflection problems," J. Rat. Mech. Anal. **5** (1956), 323–334.

[27] J. Pavageau, and J. Bousquet, "Diffraction par un réseau conducteur nouvelle méthode de résolution," Optica Acta **17** (1970), 469–478.

[28] A. Peterson, "Vector finite element formulation for scattering from two-dimensional heterogeneous bodies," IEEE Trans. Antennas Propagat. **43** (1994), 357–365.

[29] R. Petit, "A tutorial introduction," in *Electromagnetic theory of gratings*, R. Petit ed., Springer, Berlin (1980), 1–52.

[30] Petit, R. and Cadilhac, M., " Sur la diffraction d'une onde plane par un réseau infinitement conducteur," C. R. Acad. Sci. Ser. B **262** (1966), 468–471.

[31] Lord Rayleigh, "The theory of sound,", Vol. 2, Dover, New York, 1945.

[32] R. E. Scraton, "A note on the summation of divergent power series," Proc. Cambridge Philos. Soc. **66** (1969), 109–114.

[33] Talbot, D., Titchener, J. B. and Willis, J. R., "The reflection of electromagnetic waves from very rough interfaces," Wave Motion **12** (1990), 245–260.

[34] J. L. Uretsky, "The scattering of plane waves from periodic surfaces," Ann. Phys. **33** (1965), 400–427.

[35] P. M. Van den Berg, "Diffraction theory of a reflection grating," Appl. Sci. Res. **24** (1971), 261–293.

[36] P. Vincent, "Differential Methods," in *Electromagnetic theory of gratings*, ed. R. Petit, Springer, Berlin (1980), 101–121.

[37] Wait, J. R., "Perturbation analysis for reflection from two-dimensional periodic sea waves," Radio Science **6** (1971), 387–391.